

Ion-Pair Association Constant for LiOH in Supercritical Water

Andriy Plugatyr,* Ruth A. Carvajal-Ortiz, and Igor M. Svishchev

Department of Chemistry, Trent University, 1600 West Bank Drive, Peterborough, ON, Canada K9J 7B8

ABSTRACT: The equilibrium ion-pair association constant for LiOH in supercritical water is determined by means of molecular dynamics (MD) simulations via the potential of mean force calculation. Simulations are performed along three supercritical isotherms of (673.15, 773.15, and 873.15) K, covering a density range from (0.05 to 0.8) g·cm⁻³. Over the examined temperature and density range, the obtained association constant increases with increasing temperature and decreasing density. A significant increase in the association constant is observed upon transition into the low density ($\rho < \rho_c$) supercritical region. The obtained results are compared with the available experimental data at the corresponding states. To determine the corresponding states, an accurate reference equation of state for the simulated water model is used. An analytical expression for the association constant of LiOH in aqueous solution over the examined thermodynamic range is given. The results are of practical interest for chemistry control in the supercritical water-cooled nuclear reactor heat transport system.

1. INTRODUCTION

The ionization behavior of electrolytes in supercritical water is a subject of fundamental interest for hydrothermal chemistry. A significant decrease in the dielectric constant of water upon transition into low density ($\rho < \rho_c$) supercritical (LD-SCW) region promotes the formation of ion-pairs, and further ion–ion associations, at much lower concentrations than do solutions at ambient conditions. A large fraction of our knowledge of ion pairing in electrolyte solutions comes from the electrochemical (conductivity) measurements. However, the concentration range that can be accessible through these experiments is limited. Despite significant recent advances in experimental methodology,^{1–4} experimental data on the ion-pair association constants in LD-SCW are currently not available. Hence, there exists a great practical need for theoretical (computational) evaluation of the association behavior of electrolytes at high temperatures and pressures (and low densities). Noteworthy, that the theoretical, fully electrostatic models for estimation of the ion-pair association constants can fail dramatically in LD-SCW, as these primitive models do not properly account for the short-range ion–ion and ion–solvent interactions.^{5,6}

At present, molecular-based computer simulations provide the only reliable route to the ion-pair association constant in LD-SCW. In a molecular simulation, the association constant is normally determined by evaluating the radial profile of the anion–cation potential of mean force (PMF) at infinite dilution. This methodology is now well-established and has been successfully applied for the elucidation of the equilibrium behavior of a number of electrolytes in sub- and supercritical water; see refs 6–13 and therein.

The focus of this computational study is on the ionization behavior of lithium hydroxide in supercritical water over a wide range of state points, from liquid-like to gas-like. Elucidation of the ion-pair association of LiOH in supercritical water is of great practical importance for the development of chemistry control strategy for the prospective Generation IV CANDU supercritical water-cooled nuclear reactor. It is also worthwhile mentioning that in many existing pressurized water reactors operating at subcritical water conditions, LiOH is used to control the pH of the primary coolant in the heat transport system.

The ionization behavior of LiOH(aq) has been examined in a number of studies. Ion association of LiOH in dilute aqueous solution at saturation vapor pressures has been studied by Darken and Meier,¹⁴ Wright et al.,¹⁵ and Corti et al.¹⁶ Ho and Palmer² have determined ion association constants in dilute aqueous LiOH solution up to 600 °C at pressures up to 300 MPa by electrical conductance measurements in a static cell. More recently, accurate ion association constants for alkali hydroxides along the coexistence curve of water up to the critical point have been obtained by Ho et al. by using a flow-through conductivity cell.¹⁷ Unfortunately, reliable conductivity measurements in supercritical water below its critical density are extremely difficult to perform due to high degree of association of electrolytes; hence little information on the association constants is available for these conditions. Technical difficulties in obtaining accurate association constants from conductivity measurements in low density supercritical water are discussed in detail elsewhere.¹⁸

The primary goal of this study is to calculate the association constant of LiOH in supercritical water using molecular dynamics (MD) technique and to provide its easy-to-use analytical formulation, for general and engineering use. The remainder of the paper is organized as follows. The methodology and simulation details are described in Section 2. The simulation results and empirical formulation for the association constant are found in Section 3. Our conclusions are given in Section 4.

2. METHODOLOGY AND SIMULATION DETAILS

2.1. Simulation Methodology. The methodology for the determination of ion-pair association constants from molecular simulation has been described in detail elsewhere.^{6,9,10} Briefly, the ion-pair association constant, K_a , for the equilibrium



Received: May 16, 2011

Accepted: July 29, 2011

Published: August 10, 2011

is related to the infinite dilution radial distribution function (RDF) between ions, $g_{AC}^{\infty}(r)$, via:¹⁰

$$K_a = \frac{\gamma_{AC}[AC]}{\gamma_{\pm}^2[C^+][A^-]} = 4\pi \cdot R \cdot \int_0^{r_2} g_{AC}^{\infty}(r) \cdot r^2 dr \quad (2)$$

where γ is the activity coefficient, R is a numerical conversion factor to the desired units of K_a (e.g., $L \cdot mol^{-1}$), and r_2 is the boundary of the second solvation shell in the anion–cation RDF. Note that the ion association constant obtained in this fashion accounts for both contact ion pair (CIP) and solvent-shared ion pair (SSHIP) configurations. The $g_{AC}^{\infty}(r)$ can be obtained from the radial profile of the potential of mean force, $W(r)$, between ions as follows:

$$g_{AC}^{\infty}(r) = \exp\left(-\frac{W(r)}{kT}\right) \quad (3)$$

The potential of mean force is evaluated by integration of the total anion–cation mean force, $F(r)$:

$$W(r) = W(r_{\max}) - \int_{r_{\max}}^r F(r) dr \quad (4)$$

The reference mean force potential $W(r_{\max})$ is calculated by assuming the continuum limiting behavior at r_{\max} that is:

$$W(r_{\max}) \approx \frac{1}{4\pi} \frac{q_A q_C}{\varepsilon \cdot r_{\max}} \quad (5)$$

where ε is the static dielectric constant of the fluid. It is also worthwhile noting that the determination of the association constant for an electrolyte by the statistical-mechanical means requires an accurate evaluation of the dielectric constant of the modeled fluid at the respective state point.

Similarly to K_a , the equilibrium constant between CIP and SSHIP configurations, K_2 , is defined as:⁶

$$K_2 = \frac{[CIP]}{[SSHIP]} = \frac{\int_0^{r_1} g_{AC}^{\infty}(r) \cdot r^2 dr}{\int_{r_1}^{r_2} g_{AC}^{\infty}(r) \cdot r^2 dr} \quad (6)$$

where r_1 and r_2 are the boundaries of the first and second solvation shells.

2.2. Simulation Details. In this study, the simple point charge extended¹⁹ (SPC/E) model for water was employed. The thermodynamic and dielectric properties of the SPC/E model at elevated temperatures have been recently evaluated to provide accurate, reference quality equations of state²⁰ over a wide density range. This is an essential development for the present case of thermodynamic calculations as it allows one to perform the proper comparison between simulation and experimental data via the corresponding states principle. It is important to emphasize that our recent study²⁰ has shown that the SPC/E water somewhat underestimates the dielectric constant of real water. (We recall that the dielectric constant is used in the calculation of the reference PMF.) The deviations between the dielectric constant of the real²¹ and the SPC/E water are most pronounced for the high density states (see Figure 1), but below the critical density they are generally less than 5 %.

The Li^+ –water interactions were modeled by using the potential developed by Flanagan et al.²² which was optimized based on experimental and ab initio gas-phase ion–water complex data. The interaction potential for hydroxyl was taken from the study

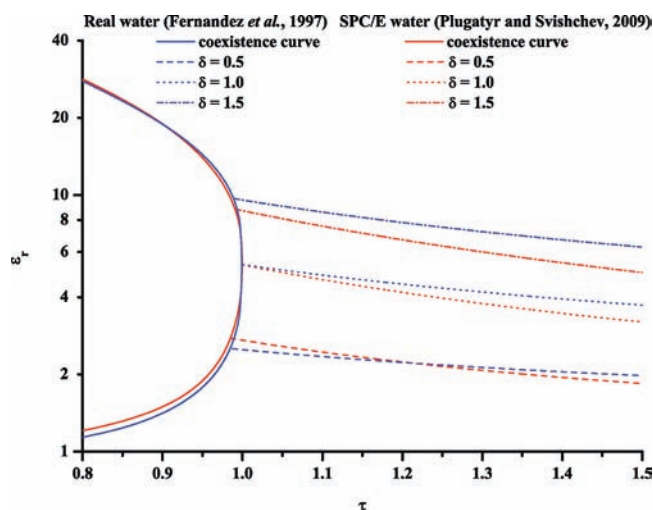


Figure 1. Comparison between the dielectric constant of real and SPC/E water, where $\delta = \rho/\rho_c$ and $\tau = T/T_c$ are the reduced density and temperature, respectively.

Table 1. Interaction Parameters of the Employed Models

model	atom	σ_{io}	ε_{io}	q/e
		Å	$kJ \cdot mol^{-1}$	
Flanagan et al. ²²	Li	2.720	0.100	1.0
Weiner et al. ²³	O	3.233	0.632	−1.3
	H	2.083	0.231	0.3
SPC/E ¹⁹	O	3.166	0.6507	−0.8476
	H			0.4238

of Weiner et al.²³ The charges and Lennard–Jones parameters of the employed models are given in Table 1. The Lorentz–Berthelot mixing rules were applied to calculate the Lennard–Jones interaction parameters for the ion pair.

In this study, we have performed the constrained dynamics simulations between spherical Li^+ and nonspherical OH^- ions by fixing the Li–O distance and allowing free rotation of the hydrogen atom of OH^- . The equations of motion were integrated by the Verlet leapfrog algorithm subject to the periodic boundary conditions in a cubic simulation cell with a time step of 2 fs. The SHAKE routine²⁴ was employed to constrain molecular geometries. The spherical cutoff radius was set at the half of the simulation cell. The simulations were performed in the NVT ensemble with temperature controlled by the Nose–Hoover thermostat.²⁵ Long-range electrostatic interactions were handled by the Ewald method. Simulations were carried out using the efficient parallel molecular dynamics code (M.DynaMix).²⁶

Simulations were performed with 510 water molecules and 1 ion pair along the three isotherms, (673.15, 773.15, and 873.15) K, over the density range of (0.05 to 0.8) $g \cdot cm^{-3}$. At the beginning of each simulation run, the ions were placed in the middle of the simulation box in the contact ion pair configuration, and the system was allowed to equilibrate for 500 ps. After the initial equilibration period, the time averages of the ion–ion and ion–solvent contribution to the potential of mean force were accumulated over 80 blocks (50 ps each) by changing the interionic distance from (1.4 to 9.4) Å with $\Delta r = 0.1$ Å. At each constrained ion-pair distance (block), the system was allowed to

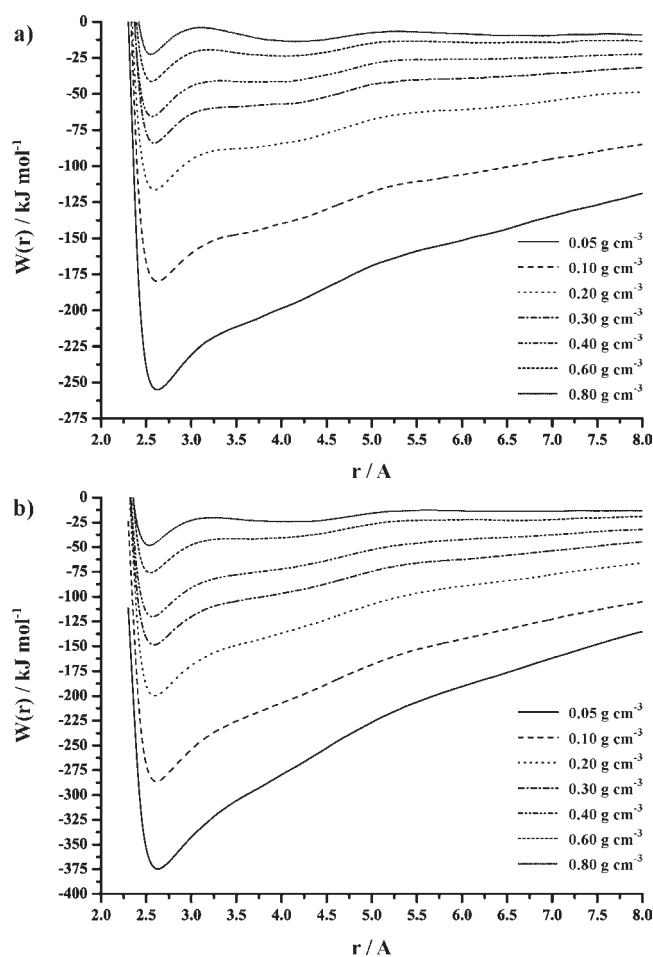


Figure 2. Radial profiles of the $\text{Li}^+ - \text{OH}^-$ potential of mean force obtained at (a) 673.15 K and (b) 873.15 K.

equilibrate for 10 ps followed by 40 ps of the mean force evaluation. The total length of each simulation run was 4500 ps. Three independent simulation runs were performed at each state point. To confirm the adapted simulation methodology, we have evaluated the ion-pair association constants for NaCl in supercritical water along the 673.15 K isotherm of the SPC/E water. The Lennard–Jones parameters for Na^+ and Cl^- were taken from Smith and Dang.²⁷ The obtained ion association constants for NaCl are in agreement with previously reported values.^{10,28}

3. RESULTS AND DISCUSSION

The radial profiles for the potentials of mean force obtained at (673.15 and 873.15) K are shown in Figure 2. The first and second minima of the PMF profiles reflect the geometry and stability (well depth) of the CIP and the SShIP configurations. In Figure 3, we display the corresponding radial distribution functions obtained at 673.15 K. This figure clearly illustrates boundaries of the first and second solvation shells for the $\text{Li}^+ - \text{OH}^-$ ion pair in dense supercritical water. The ions in CIP and SShIP configurations are separated by (2.7 and 4.1) Å, with the minima in pair density being at about (3.2 and 5.25) Å, respectively (these minima are treated as the boundaries of the solvation shells). The distance between ions in the CIP configuration appears to be independent of the state conditions examined in

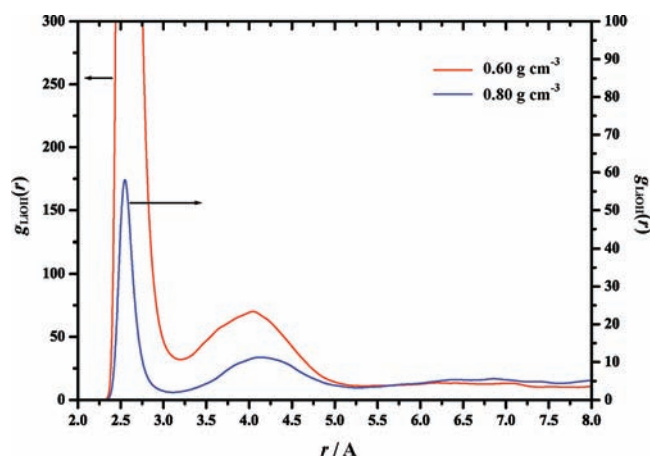


Figure 3. Radial distribution functions for $\text{Li}^+ - \text{OH}^-$ ion pair in infinitely dilute aqueous solution at 673.15 K.

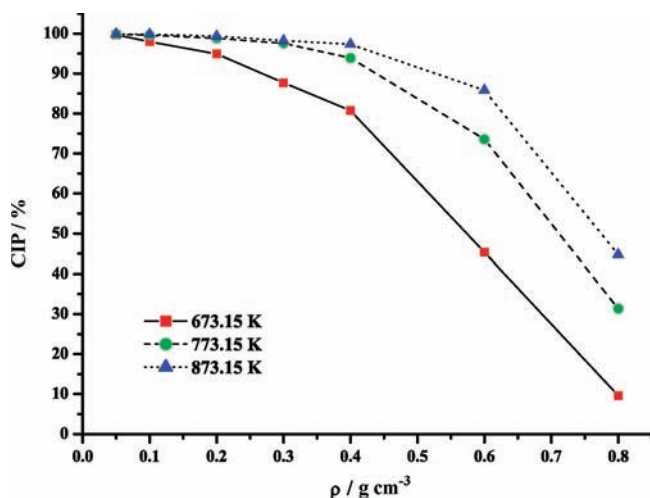


Figure 4. Relative concentration of ion pairs in the CIP configuration.

Table 2. Logarithm of Molar Association Constants, $\log_{10}K_a(M)$, of Aqueous LiOH Solution

ρ $\text{g} \cdot \text{cm}^{-3}$	T/K		
	673.15	773.15	873.15
0.05	17.84 ± 0.26	20.03 ± 0.28	20.48 ± 0.06
0.1	12.06 ± 0.28	14.34 ± 0.30	15.18 ± 0.25
0.2	7.15 ± 0.22	8.86 ± 0.15	10.01 ± 0.10
0.3	4.65 ± 0.07	6.16 ± 0.23	6.97 ± 0.30
0.4	3.22 ± 0.08	4.41 ± 0.08	5.25 ± 0.10
0.6	1.48 ± 0.07	2.19 ± 0.21	2.65 ± 0.12
0.8	0.44 ± 0.04	0.85 ± 0.19	1.17 ± 0.16

this study. As expected, the stability of the CIP configuration increases with decreasing density and increasing temperature. In contrast, the stability of the SShIP configuration decreases with decreasing density and increasing temperature. The fraction of CIP configurations as a function of density along the three isotherms is plotted in Figure 4. As can be seen from this figure, at $0.8 \text{ g} \cdot \text{cm}^{-3}$ the CIP configurations account for about (10, 31, and 45) % at

Table 3. Logarithm of Molar Equilibrium Constants, $\log_{10}K_2(M)$, between the CIP and SShIP Configurations (from eq 6) for LiOH in Aqueous Solution

ρ g·cm ⁻³	T/K		
	673.15	773.15	873.15
0.05	2.56 ± 0.17	2.85 ± 0.04	3.06 ± 0.07
0.1	1.73 ± 0.14	2.41 ± 0.04	2.73 ± 0.13
0.2	1.29 ± 0.10	1.93 ± 0.06	2.20 ± 0.05
0.3	0.89 ± 0.15	1.61 ± 0.05	1.77 ± 0.12
0.4	0.62 ± 0.04	1.20 ± 0.07	1.58 ± 0.10
0.6	-0.07 ± 0.12	0.46 ± 0.09	0.79 ± 0.09
0.8	-0.97 ± 0.06	-0.34 ± 0.08	-0.09 ± 0.01

Table 4. Fitting Parameters to eq 7

i	a_i
1	15.691
2	-11.590
3	-23.587
4	12.112
5	-7.958
6	14.404

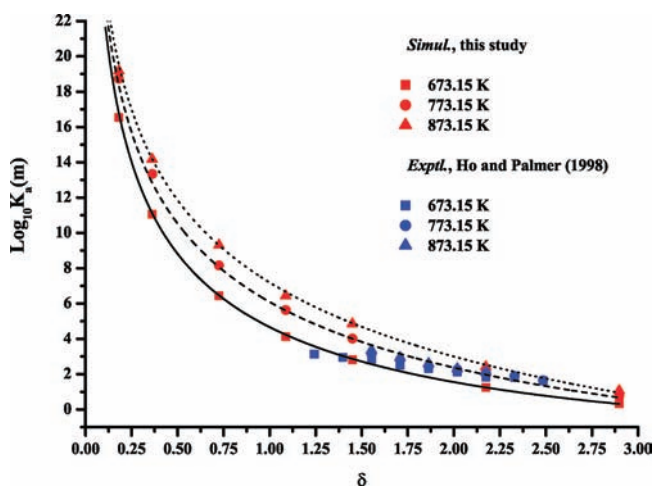


Figure 5. Molal ion-pair association constants of LiOH in aqueous solution. Lines represent fitted values from eq 7.

(673.15, 773.15, and 873.15) K, respectively. Coincidentally, at this density the SShIP fraction appears to be independent of temperature and amounts to approximately 30 %. The remaining solvent-separated ion pairs (SSIP) contribute (61, 40, and 28) % at (673.15, 773.15, and 873.15) K, respectively. As density decreases, the fraction of ions in the CIP configuration increases dramatically as the critical density is approached and passed. Thus, at 0.4 g·cm⁻³ and 673.15 K, more than 80 % of the total configurations are CIP. It is interesting to note that at this density virtually all ion pairs are either CIP or SShIP, where the SShIP configurations account for about (15, 6, and 3) % at (673.15, 773.15, and 873.15) K, respectively. Below the critical density of the SPC/E water ($\rho_c = 0.276$ g·cm⁻³)²⁰ more than 95 % are CIP.

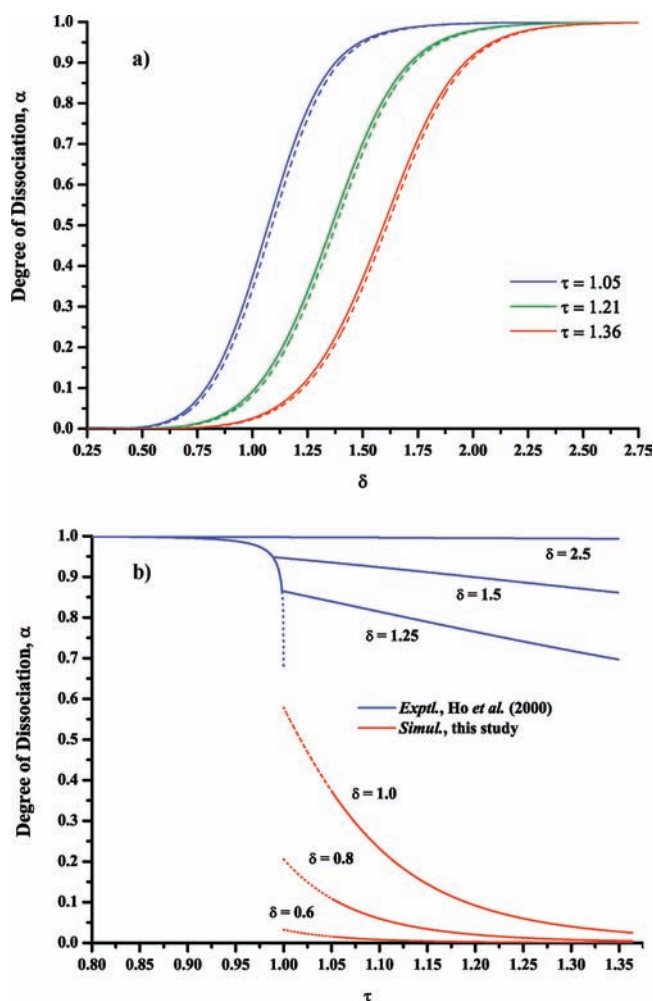


Figure 6. (a) Degree of dissociation of LiOH in a 10⁻⁴ mol·kg⁻¹ aqueous solution as a function of reduced density along three supercritical isotherms. Solid lines represent the degree of dissociation calculated assuming unity activity coefficients. The effect of the ionic strength on the degree of dissociation is shown with dashed lines. (b) Degree of dissociation of LiOH in a 10⁻⁴ mol·kg⁻¹ aqueous solution as a function of reduced temperature along several selected isochors. Dashed lines represent extrapolation.

The obtained overall ion association, K_a , and CIP/SShIP, K_2 , constants for LiOH in aqueous solution are given in Tables 2 and 3, respectively. Equations 2 to 6 were employed, together with the values for the dielectric constant taken from the reference dielectric equation of state for the SPC/E potential.²⁰ In this study, the values of the molal ion association constant, $K_a(m) = \rho \cdot K_a$, for LiOH were fitted by using an empirical equation similar to the commonly used “density” model:¹⁷

$$\log_{10}K_a(m) = a_1 + \frac{a_2}{\tau} + \left(a_3 + \frac{a_4}{\tau}\right) \cdot \log_{10}\delta + \left(a_5 + \frac{a_6}{\tau}\right) \cdot (\log_{10}\delta)^2 \quad (7)$$

where $\delta = \rho/\rho_c$ and $\tau = T/T_c$ are the reduced density and temperature, respectively. The mean relative error of the fit was estimated to be 2.64 %. The fitting parameters to eq 7 are given in Table 4.

In Figure 5, our simulation results for the ion-pair association constant for LiOH are compared with available experimental data as a function of reduced density. Figure 4 indicates a very good agreement between the constant of association obtained in this study and the results from electrical conductance measurements.² Thus, the predicted $\log_{10}K_a(m)$ values of 1.75, 2.65, and 3.35 obtained from eq 7 compare very well with the corresponding experimental results of 2.32, 2.43, and 2.75 obtained by Ho and Palmer² at $0.6 \text{ g} \cdot \text{cm}^{-3}$ and (673.15, 773.15, and 873.15) K, respectively. As can be seen from Figure 4, $\log_{10}K_a(m)$ values exhibit a strong isothermal density dependence. A significant increase in the molal association constant of LiOH is observed below the critical density. The $\log_{10}K_a(m)$ increases from 2.87 (673.15 K) and 4.89 (873.15 K) at $0.4 \text{ g} \cdot \text{cm}^{-3}$ to 16.78 (673.15 K) and 19.54 (873.15 K) at $0.05 \text{ g} \cdot \text{cm}^{-3}$. A similar behavior of the association constants for NaCl and HCl in low density supercritical states was reported previously.^{5,12}

The degree of dissociation (eq 5, in ref 10) of $10^{-4} \text{ mol} \cdot \text{kg}^{-1}$ solution of LiOH is plotted in Figure 6. This figure illustrates a rapid decrease of the degree of the dissociation upon transition into low density supercritical states. Our results indicate that below $\delta = 0.5$ more than 99.6 % of LiOH ions in 10^{-4} molal LiOH solution associate.

Obtained results are useful not only for analyzing electrolyte behavior at extreme conditions, where experimental measurements are scarce, but also provide a simple means to estimate the pH for industrially relevant high temperature LiOH solutions. One of their main applications is in nuclear power cycle chemistry control and corrosion prevention.

4. CONCLUSIONS

The ionization behavior of LiOH in supercritical water has been examined over a wide temperature and density range by means of molecular dynamics simulation. The obtained ion-pair association constants for LiOH agree well with available experimental data at the corresponding state points of high density. An analytical expression describing the behavior of the association constant of LiOH in aqueous solution over the examined thermodynamic range is presented. A significant increase in the ion association constant for LiOH is observed upon transitions into low density ($\rho < \rho_c$) supercritical states, where CIP configurations account for more than 95 % of all ion pairs.

AUTHOR INFORMATION

Corresponding Author

*E-mail: andriyplugatyr@trentu.ca.

Funding Sources

This work was made possible by the facilities of the Shared Hierarchical Academic Research Computing Network (SHARCNET: www.sharcnet.ca) and Comput/Calcul Canada. The authors are grateful for the financial support of the NSERC/NRCan/AECL Generation IV Energy Technologies Program and SHARCNET.

REFERENCES

(1) Zimmerman, G. H.; Gruszkiewicz, M. S.; Wood, R. H. New Apparatus for Conductance Measurements at High-Temperatures - Conductance of Aqueous-Solutions of LiCl, NaCl, NaBr, and CsBr at 28 MPa and Water Densities from 700 to 264 kg m^{-3} . *J. Phys. Chem.* **1995**, *99*, 11612–11625.

(2) Ho, P. C.; Palmer, D. A. Determination of ion association in dilute aqueous lithium chloride and lithium hydroxide solutions to 600 °C and 300 MPa by electrical conductance measurements. *J. Chem. Eng. Data* **1998**, *43*, 162–170.

(3) Ho, P. C.; Bianchi, H.; Palmer, D. A.; Wood, R. H. Conductivity of dilute aqueous electrolyte solutions at high temperatures and pressures using a flow cell. *J. Solution Chem.* **2000**, *29*, 217–235.

(4) Erickson, K. M.; Arcis, H.; Raffa, D.; Zimmerman, G. H.; Tremaine, P. R. Deuterium Isotope Effects on the Ionization Constant of Acetic Acid in H₂O and D₂O by AC Conductance from 368 to 548 K at 20 MPa. *J. Phys. Chem. B* **2011**, *115*, 3038–3051.

(5) Chialvo, A. A.; Simonson, J. M. Aqueous Na⁺Cl⁻ pair association from liquidlike to steamlike densities along near-critical isotherms. *J. Chem. Phys.* **2003**, *118*, 7921–7929.

(6) Chialvo, A. A.; Cummings, P. T.; Simonson, J. M. H₃O⁺/Cl⁻ ion pairing in hydrothermal solutions by simulation and electrical conductance. A review. *J. Mol. Liq.* **2003**, *103*, 235–248.

(7) Cui, S. T.; Harris, J. G. Ion Association and Liquid Structure in Supercritical Water Solutions of Sodium-Chloride - a Microscopic View from Molecular-Dynamics Simulations. *Chem. Eng. Sci.* **1994**, *49*, 2749–2763.

(8) Gao, J. L. Simulation of the Na⁺Cl⁻ Ion-Pair in Supercritical Water. *J. Phys. Chem.* **1994**, *98*, 6049–6053.

(9) Chialvo, A. A.; Cummings, P. T.; Cochran, H. D.; Simonson, J. M.; Mesmer, R. E. Na⁺-Cl⁻ Ion-Pair Association in Supercritical Water. *J. Chem. Phys.* **1995**, *103*, 9379–9387.

(10) Chialvo, A. A.; Cummings, P. T.; Simonson, J. M.; Mesmer, R. E. Temperature and density effects on the high temperature ionic speciation in dilute Na⁺/Cl⁻ aqueous solutions. *J. Chem. Phys.* **1996**, *105*, 9248–9257.

(11) Chialvo, A. A.; Ho, P. C.; Palmer, D. A.; Gruszkiewicz, M. S.; Cummings, P. T.; Simonson, J. M. H₃O⁺/Cl⁻ association in high-temperature aqueous solutions over a wide range of state conditions. A direct comparison between simulation and electrical conductance experiment. *J. Phys. Chem. B* **2002**, *106*, 2041–2046.

(12) Chialvo, A. A.; Simonson, J. M. H₃O⁺Cl⁻ pair association in steam and highly compressible aqueous environments. *J. Phys. Chem. C* **2007**, *111*, 15569–15574.

(13) Chialvo, A. A.; Gruszkiewicz, M. S.; Cole, D. R. Ion-Pair Association in Ultrasupercritical Aqueous Environments: Successful Interplay among Conductance Experiments, Theory, and Molecular Simulations. *J. Chem. Eng. Data* **2010**, *55*, 1828–1836.

(14) Darken, L. S.; Meier, H. F. Conductances of Aqueous Solutions of the Hydroxides of Lithium, Sodium and Potassium at 25 °C. *J. Am. Chem. Soc.* **1942**, *64*, 621–623.

(15) Wright, J. M.; Lindsay, W. T., Jr.; Druga, T. R. *The behavior of electrolytic solutions at elevated temperatures as derived from conductance measurements*; WAPD-TM-204; Westinghouse, Tech. Service, Dept. of Commerce: Washington, DC, 1961.

(16) Corti, H.; Crovetto, R.; Fernández-Prini, R. Aqueous solutions of lithium hydroxide at various temperatures: Conductivity and activity coefficients. *J. Solution Chem.* **1979**, *8*, 897–908.

(17) Ho, P. C.; Palmer, D. A.; Wood, R. H. Conductivity measurements of dilute aqueous LiOH, NaOH, and KOH solutions to high temperatures and pressures using a flow-through cell. *J. Phys. Chem. B* **2000**, *104*, 12084–12089.

(18) Ho, P. C.; Palmer, D. A.; Gruszkiewicz, M. S. Conductivity measurements of dilute aqueous HCl solutions to high temperatures and pressures using a flow-through cell. *J. Phys. Chem. B* **2001**, *105*, 1260–1266.

(19) Berendsen, H. J. C.; Grigera, J. R.; Straatsma, T. P. The missing term in effective pair potentials. *J. Phys. Chem.* **1987**, *91*, 6269–6271.

(20) Plugatyr, A.; Svishchev, I. M. Accurate thermodynamic and dielectric equations of state for high-temperature simulated water. *Fluid Phase Equilib.* **2009**, *277*, 145–151.

(21) Fernandez, D. P.; Goodwin, A. R. H.; Lemmon, E. W.; Sengers, J. M. H. L.; Williams, R. C. A Formulation for the Static Permittivity of Water and Steam at Temperatures from 238 to 873 K at Pressures up to 1200 MPa, Including Derivatives and Debye-Hückel Coefficients. *J. Phys. Chem. Ref. Data* **1997**, *26*, 1125–1166.

(22) Flanagan, L. W.; Balbuena, P. B.; Johnston, K. P.; Rossky, P. J. Ion solvation in supercritical water based on an adsorption analogy. *J. Phys. Chem. B* **1997**, *101*, 7998–8005.

(23) Weiner, S. J.; Kollman, P. A.; Nguyen, D. T.; Case, D. A. An all Atom Force-Field for Simulations of Proteins and Nucleic-Acids. *J. Comput. Chem.* **1986**, *7*, 230–252.

(24) Ryckaert, J. P.; Ciccotti, G.; Berendsen, H. J. C. Numerical-Integration of Cartesian Equations of Motion of a System with Constraints - Molecular-Dynamics of N-Alkanes. *J. Comput. Phys.* **1977**, *23*, 327–341.

(25) Nose, S. A molecular dynamics method for simulations in the canonical ensemble. *Mol. Phys.* **2002**, *100*, 191–198.

(26) Lyubartsev, A. P.; Laaksonen, A. MDynaMix - a scalable portable parallel MD simulation package for arbitrary molecular mixtures. *Comput. Phys. Commun.* **2000**, *128*, 565–589.

(27) Smith, D. E.; Dang, L. X. Computer-Simulations of NaCl Association in Polarizable Water. *J. Chem. Phys.* **1994**, *100*, 3757–3766.

(28) Yui, K.; Sakuma, M.; Funazukuri, T. Molecular dynamics simulation on ion-pair association of NaCl from ambient to supercritical water. *Fluid Phase Equilib.* **2010**, *297*, 227–235.